Breast Cancer Risk Estimation using Patient Health Information and Tactile Sensing System

Sung In Choi[1], Dina Caroline[2], Chang-hee Won[1]
[1]Electrical and Computer Engineering Dept., Temple University Engineering, Philadelphia, USA
[2]Radiology Dept., Temple University Hospital, Philadelphia, USA

***Abstract* — Developing an accurate estimation of risk in the early stage of breast cancer increases the prognosis of the disease and awareness of the personal risk of having invasive breast cancers in the lifetime. In this paper, we present the breast cancer risk estimation method to compute the relative total risk score using Tactile Sensing System and patient health information. The main breast cancer risk is estimated by the malignancy risk index from the mechanical properties of the mass, which is obtained by tactile images. Then, the risk score is computed by combining the personal breast cancer risk based on the patient's age and race information. The method was applied to 7 human cases and resulted in 86.0% accuracy in detecting malignant tumors.**

Keywords—breast cancer risk estimation, breast lesion malignancy risk, non-invasive sensing, patient health record, Tactile Sensing System

I. INTRODUCTION

Global cancer statistics estimated 2.3 million new cases of female breast cancer in 2019, and it is the fifth leading cause of cancer deaths [1]. However, breast cancer patient has a high chance of survival if detected early [2]. The risk prediction alerts a woman to get a breast checkup and monitor any abnormality in the breast. Over the years, various prediction models for breast cancer risk have been developed, improving breast cancer mortality rate [3], [4]. The models utilize the patient's health record, typically age, race, family, medical history, and genetic information. The prediction accuracy of the models increases proportionally when more detailed information is available [3], [4]. Sometimes, we do not have all these medical health data. Thus, a research group [5] developed a simpler breast cancer risk model using age, race, and breast density information. More recently, researchers have proposed race and ethnicity-based risk assessment models. The Gail model is one of the most popular and earlier developed models [5], but it requires extensive family and medical health data, including ethnicity [6]-[8]. Our proposed method utilizes the study [5] to develop a simple risk prediction method.

The physical examination result provides an additional factor in estimating breast cancer risk, particularly in women who have a palpable lump in their breast tissue. Even if the detected lump is benign, such as atypical ductal hyperplasia (ADH), it requires monitoring [9] since the mass could become breast cancer. Having a benign lump increases the risk 10-fold. Thus, the risk estimation of the detected mass will help manage the risk effectively. The tactile imaging technique is an objective and non-invasive examining tool for the breast mass [10] – [12] compared to the subjective clinical breast examination [13], [14].

Our proposed Tactile Sensing System is designed to perform the clinical breast examination in an objective and quantifiable manner. In this paper, we will discuss the methods and results of breast cancer risk estimation using patient health records and physical examination using the Tactile Sensing System (TSS).

II. BREAST CANCER RISK ESTIMATION

Breast cancer risk estimation (BCRE) is a method to determine a woman's relative risk of having breast cancer. We compute the personal breast cancer risk using the patient's health record (age and race) and the lesion malignancy risk index using the Tactile Sensing System, as shown in Fig. 1.

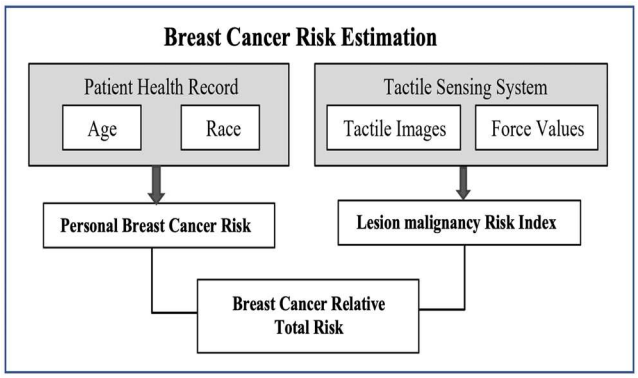

Fig. 1. Overview of Breast Cancer Risk Estimation

A. Tactile Sensing System

Tactile Sensing System (TSS) is a human palpation-mimicking sensor designed for clinical breast examination. The sensor is developed and used for lesion characterization [18] and [19], which uses the basic principle of the light reflection inside the transparent and soft optical waveguide made of polydimethylsiloxane (PDMS). The probe reads the light scattering pattern once the surface of the optical waveguide is touched. The soft PDMS tip is deformed, and the light pattern changes corresponding to the amount of applied force and area of deformation.

The probe consists of a CCD camera (Guppy F-038, Allied Vision Technologies, Exton, PA), a force sensor (Compression load cell FC22, TE Connectivity), a controller circuit, and the sensing tip. The sensing tip contacts and examines the tissue directly. The tip is made of Polydimethylsiloxane (PDMS) (20mm x 23mm x 14mm), and the LED light source (four ultra-bright white light-emitting diodes) injects the light into the tip.

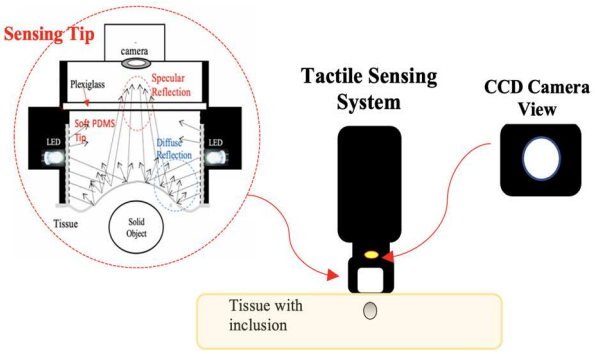

Fig. 2. Tactile Sensing System schematic and sensing principle

Fig. 2 shows the TSS sensing principle and operation concept. The probe applies a specific force range to the target tissue, inducing the deformation of the tissue and the sensing tip. In this process, the light rays distributed inside the sensing tip create different amounts of pixel intensity captured by the image sensor. The amount of intensity change is directly proportional to the tissue's stiffness change due to the embedded mass hardness at the constant applying force. Thus, the relationship is characterized by estimating the tissue stiffness level.

B. Patient Health Record-based Risk Assessment

Breast cancer risk is assessed with many prediction models of breast cancer risk. The prediction models are used to define the individual's probability of having breast cancer in a certain period of a lifetime [15]. As mentioned, the prediction value is computed based on the patient's medical and family history. In BCRE, we calculate the current personal breast cancer risk, which uses only age and race to generate a reasonable discriminator of the risk level. This will enhance the user's accessibility and reduce the computational cost.

In [5], the simplified Gail model predicts individualized risk prediction using limited information about patients. The incidence model presented in the study uses only the age and race of the patient. The incidence model, a 3rd order polynomial derived based on age and race from the cases in the 1998 to 2002 SEER invasive breast cancer dataset [16], [17] and the hazardous factor based on the breast density are mainly used to get the probability in this study [5]. The breast cancer incidence value (per 100,000) is estimated from the following equation,

$$I_{x,r} = a_r x^3 + b_r x^2 + c_r x + d_r \quad (1)$$

The $I_{x,r}$ value provides the risk distribution among the age, x in the four race/ethnicity groups, r, r=w (White), $r = b$ (Black), $r = a$ (Asian), $r = h$ (Hispanic), which is a part of the patient health record [5]. We calculate the personal breast cancer risk of the patient based on the incident model (1).

III. METHODOLOGY

A. Lesion Malignancy Risk Index

The lesion malignancy risk index is calculated using the TSS images and the corresponding applied forces. We preprocess the obtained tactile images of the area of interest (ROI). The images of the healthy breast tissue region and the lesion should be taken on the same breast as the applying force increases from $7 \pm 2.5N$ to $20 \pm 2.5N$. Then we obtain the sum of the pixel intensity in the region ROI and the applying forces of the images. The intensity sum gradually increases as the applied force increases. The stiffness level of the breast tissue (S_m for mass-embedded tissue, S_h for healthy tissue),

$$S_{m\ or\ h} = \frac{\sum_{i=1}^{n}(M_i - \overline{M})(F_i - \overline{F})}{\sum_{i=1}^{n}(F_i - \overline{F})^2} \quad (2)$$

is the slope of the linear regression among the data in the specified force range, which indicates how much intensity grows when force increases. In (2), M_i is the pixel intensity sum in the ROI of i^{th} image, and $\overline{M}$ is the average of M_i values. F_i is the corresponding applied force of each image taken, and $\overline{F}$ is the average of all forces in the range. Now we calculate the lesion malignancy risk index,

$$R_l = \frac{S_m}{S_h} \quad (3)$$

which is the stiffness ratio between the lesion and the healthy tissue. The ratio-based assessment is formulated based on our previous work on the smartphone version's data processing method [21].

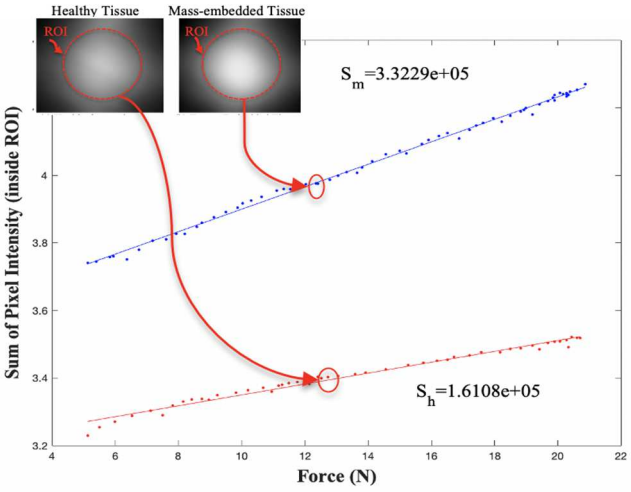

Fig. 3. Example of stiffness level values from one of the human breast tissue data– malignant case (Red: healthy breast tissue, Blue: mass-embedded breast tissue)

We define the stiffness values of the healthy and mass-embedded sites of the breast tissue using (2). The case in Fig. 3 exhibits the expected relation of the hard tumor inside the tissue to the healthy tissue. Each data point is computed based on the TSS images of the healthy tissue and the mass-embedded tissue, as shown in Fig. 3. For the malignant case, we observed that the S_m value is almost twice larger than S_h. It shows that the malignant tumor is stiffer than the other tissues, as stated in [22] and [23]. Thus, we can define that the malignancy risk of the lesion is high in this case based on the physical assessment risk. This index is used to compute the relative total risk.

B. Personal Breast Cancer Risk

Personal breast cancer risk indicates the patient's risk of developing breast cancer at a certain age compared to the

base risk value, β_r, using the expected value in [20] as follows.

$$\beta_r = \sum_{x=min}^{max} p_{x,r}\, I_{x,r} \tag{4}$$

where $I_{x,r}$ is the incidence value from (1). Intuitively, β_r is the average of all $I_{x,r}$ for the selected age range and for the specific race over the entire age range for that race. β_r would serve as a basis to assess high or low personal breast cancer risk. $p_{x,r}$ is the probability mass function defined by

$$p_{x,r} = \frac{1}{I_{tot}} \tag{5}$$

where the count of each incidence value at age is always one in our case because the incidence value is unique for each age group. I_{tot} is the total number of incidence values in the selected age range and for the specific race ($I_{tot} = x_{max} - x_{min} + 1$). $p_{x,r}$ is always $\frac{1}{66}$, where the maximum age (x_{max}) is 100, and the minimum age (x_{min}) is 35. The sum of all $p_{x,r}$ is one as in [20]. Now we define the personal breast cancer risk as

$$R_s = {I_{x_p,r}}/{\beta_r} \tag{6}$$

where x_p is the patient's age, and r is the race. If R_s is greater than one, then this means that the woman at that age has a higher risk of breast cancer than the base value, β_r, in the same ethnicity group as shown in Fig. 4. β_r is calculated for four groups: β_w for White, β_b for Black, β_a for Asian, and β_h for Hispanic group.

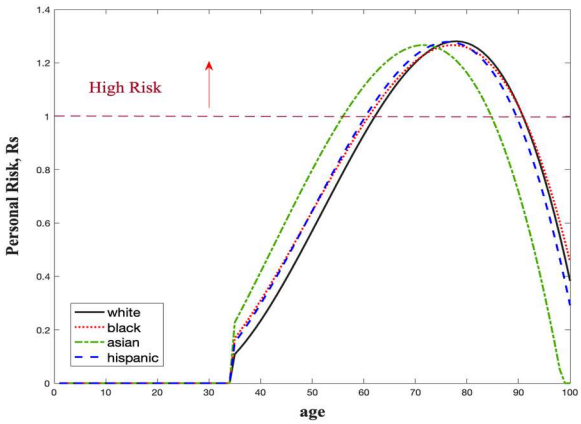

Fig. 4. Personal breast cancer risk models of women ages (35–100) in four different race groups

Fig. 4 demonstrates the personal risk models of four races. The models show the R_s values over age. In our method, we consider the age below 35 as a zero value in the calculation since young women have a very low possibility of breast cancer [16]. A high-risk case is indicated if the patient has a value over one. We incorporate this risk value with the physical malignancy risk index to estimate the relative total risk.

C. Relative Total Risk

Relative total risk is a numeric score value of the woman's breast cancer risk level (who has a lesion). To compute the score, we incorporate the personal breast cancer risk of the person at the age and the lesion's malignancy risk index. The patient's relative total risk of breast cancer,

$$R_{total} = (\varphi_1 R_{sn} + \varphi_2 R_{ln}) \tag{7}$$

is the weighted sum of R_{sn} and R_{ln}, the normalized R_s from (6) and R_l from (3). We normalize each risk value based on the maximum and minimum possible risk values to combine them into one scale. Then, the normalized risk values are weighted by φ_1 and φ_2.

IV. Results

To verify the proposed method, we applied the method to seven female patients. We obtained biopsy results from the Temple University Hospital Radiology Department. Table I shows the risk estimation result of the human patients. To estimate the relative total risk (7), we applied the weight of 0.5 for φ_1 and φ_2. The risk was considered if the value was greater and equal to 0.5 (≥50% of the normal state). The risk estimation for the human data resulted in 86.0% accuracy in discriminating malignant (high risk) and benign (low risk) cases with 100.0% sensitivity and 80.0% specificity (** refers to the false positive case from the estimation). Its sensitivity is higher than the digital mammogram sensitivity 86.9% of [24].

TABLE I. Risk Values of Human Data and Malignancy Risk Assessment (High Risk of Malignant Breast Tumor if R≥0.5)

Patient	R_{sn}	R_{ln}	R_{total}	Estimated Risk Level	Biopsy Result
1	0.45	0.34	0.40	low	Benign
2	0.24	0.52	0.38	low	Benign
3	0.93	0.60	0.77	high	Malignant
4	0.00	0.05	0.03	low	Benign
5	0.56	0.21	0.39	low	Benign
6	0.64	1.00	0.82	**high	Benign
7	0.96	0.69	0.83	high	Malignant

V. Conclusion

In this paper, we presented the breast cancer risk estimating method that uses the simple patient health record and the TSS data of a breast mass. We obtained 86% accuracy and 100% sensitivity. This sensitivity was higher than the digital mammogram. We conclude that this BCRE method has a high potential to estimate breast cancer risk accurately. However, this study was for a small patient sample, and we need a more extensive scale dataset in the future to confirm the utility of the risk estimation method.

Acknowledgment

The authors thank Vira Oleksyuk and Suzanne Pascarella for their help in Tactile Sensing System development and human data collection. The authors thank Arpita Das for editing the draft. This work was supported in part by the National Science Foundation's ECCS-2114675.

REFERENCES

[1] H. Sung *et al.*, "Global cancer statistics 2020: GLOBOCAN estimates of incidence and mortality worldwide for 36 cancers in 185 countries," in *CA Cancer J Clin.* vol. 71, pp. 209-249, May/Jun 2021. [Online]. Available: https://doi.org/10.3322/caac.21660

[2] A. B. Nover et al., "Modern Breast Cancer Detection: A Technological Review," *International Journal of Biomedical Imaging*, vol. 2009, article 902326, pp. 1-4, Jan. 2009.

[3] D. G. R. Evans and A. Howell, "Breast cancer risk-assessment models," Breast Cancer Res., vol. 9, no. 5, pp. 1–8, 2007.

[4] E. Amir, O. C. Freedman, B. Seruga, and D. G. Evans, "Assessing Women at High Risk of Breast Cancer: A Review of Risk Assessment Models," *JNCI: Journal of the National Cancer Institute*, vol. 102, no. 10, pp. 680-691, 2010.

[5] J. A. Tice, S. R. Cummings, R. Smith-Bindman, L. Ichikawa, W. E. Barlow, and K. Kerlikowske, "Using clinical factors and mammographic breast density to estimate breast cancer risk: development and validation of a new predictive model," *Annals of internal medicine*, vol.148, no. 5, pp.337–347, 2008.

[6] S. Rostami, A. Rafei, M. Damghanian, Z. Khakbazan, F. Maleki, and K. Zendehdel, "Discriminatory Accuracy of the Gail Model for Breast Cancer Risk Assessment among Iranian Women." *Iranian J Public Health*, vol. 49, no. 11, pp. 2205–2213, 2020. https://doi.org/10.18502/ijph.v49i11.4739

[7] B. Park *et al.*, "Korean risk assessment model for breast cancer risk prediction." *PloS one*, vol. 8, no.10, e76736, 2013.

[8] C. E. Jacobi, G. H. de Bock, B. Siegerink, and C. J. van Asperen, "Differences and similarities in breast cancer risk assessment models in clinical practice: which model to choose?" *Breast Cancer Res. Treat.*, vol. 115, no. 2, pp. 381–390, 2009.

[9] L. C. Hartman *et al.*, "Atypical Hyperplasia of the Breast — Risk Assessment and Management Options," *N Engl J Med*., vol.3 72, no. 1, pp. 78–89, 2015.

[10] C.-H. Won, J.-H. Lee, and F. Saleheen, "Tactile Sensing Systems for Tumor Characterization: A Review," *IEEE Sens. J.*, vol. 21, no. 11, pp.12578–12588, May 2021.

[11] P. S. Wellman, E. P. Dalton, D. Krag, K. A. Kern, R. D, Howe. "Tactile Imaging of Breast Masses: First Clinical Report," *Arch Surg*. vol.136, no.2, pp. 204–208, 2001.

[12] C. Van Nguyen, & R. F. Saraf, "Tactile imaging of an imbedded palpable structure for breast cancer screening," *ACS applied materials & interfaces*, vol.6, no.18, pp. 16368–16374, 2014.

[13] T. Ratanachaikanont, "Clinical breast examination and its relevance to diagnosis of palpable breast lesion," *J. of the Medical Association of Thailand*, vol.88, no.4, pp.505-507, 2005.

[14] F. Demirkiran, N. A. Balkaya, S. Memis, G. Turk, S. Ozvurmaz, and P. Tuncyurek, "How do nurses and teachers perform breast self-examination: are they reliable sources of information?" *BMC Public Health*, vol.7, article 96, 2007.

[15] A. R. Brentnall, & J. Cuzick, "Risk Models for Breast Cancer and Their Validation," *Statistical science: a review journal of the Institute of Mathematical Statistics*, vol. 35, no. 1, pp. 14–30, 2020.

[16] M. Kamińska, T. Ciszewski, K. Łopacka-Szatan, P. Miotła, and E. Starosławska, "Breast cancer risk factors. Przeglad menopauzalny = Menopause review," vol. 14, no. 3, pp. 196–202, 2015.

[17] N. Howlader *et al.*(eds), "SEER Cancer Statistics Review, 1975-2016," National Cancer Institute. Bethesda, MD, April 9, 2020, [Online]. Available: https://seer.cancer.gov/csr/1975_2016/.

[18] J.-H. Lee and C.-H. Won, "High-resolution tactile imaging sensor using total internal reflection and nonrigid pattern matching algorithm," *IEEE Sensors J.*, vol. 11, no. 9, pp. 2084–2093, Sep. 2011

[19] J.-H. Lee and C.-H. Won, "The Tactile Sensation Imaging System for Embedded Lesion Characterization," *IEEE J. of Biomedical and Health Informatics*, vol. 17, no. 2, pp. 2168–2194, Mar. 2013.

[20] R. D. Yates and D. J. Goodman, "Discrete random variable," in *Probability and Stochastic Processes: A Friendly Introduction for Electrical and Computer Engineers*. United Kingdom: Wiley, 2014, pp. 62-99.

[21] S. Choi, V. Oleksyuk, D. Caroline, S. Pascarella, R. Kendzierski, and C.-H. Won, "Breast Tumor Malignancy Classification using Smartphone Compression-induced Sensing System and Deformation Index Ratio," *42nd Annu. Int. Conf. IEEE Eng. Med. Biol. Soc. (EMBC)*, Montr. QC, Canada, 2021, pp. 6082–6085.

[22] T. A. Krouskop, T. M. Wheeler, F. Kallel, B. S. Garra, and T. Hall, "Elastic Moduli of Breast and Prostate Tissues under Compression," *Ultrasonic Imaging*, vol.20, no.4, pp.260-274, Oct. 1998.

[23] M. J. Paszek et al., "Tensional homeostatsis and the malignant phenotype," *Cancer Cell*, vol.8, no.3, pp.241-254, Sep. 2005.

[24] C. D. Lehman *et al*. "National performance benchmarks for modern screening digital mammography: update from the Breast Cancer Surveillance Consortium," *Radiology*. vol.283, no.1, pp. 49–58, Apr. 2017.